

EVALUATION OF LONG-SHORE SEDIMENT TRANSPORT ON THE KUNDUCHI BEACH TIDAL FLAT, DAR ES SALAAM

Alfonse M. Dubi
Institute of Marine Sciences, University of Dar es Salaam
P.O. Box 668 Zanzibar, Tanzania

Kunduchi Beach is located approximately 10 kilometres north of Dar es Salaam City on the coast of Mainland Tanzania. Currents and sediment concentrations were measured using a multi-sensor self-recording current meter. Waves were measured using pressure gauges. Some physical features were visually measured.

The general orientation of the shoreline is 330 degrees and the tidal flat is characterised by ripples. At about 150 m from the shoreline, ripples are 7-9 cm high and their wavelength is about 40 cm. Closer to the beach, ripple orientation is 350 degrees; ripple height is 5 cm and ripple wave length is 5 cm.

Results from the measurements show that during flood tide the current direction is southerly (an average of 210 degrees) and at high tide the average direction is 150 degrees. The direction of the ebb tidal current is northerly (an average of 360 degrees). On the average, the current speed was 0.1 m/s. Significant waves heights increased with increasing water level, from 0.1 metres in water depth of 0.5 metres to about 0.4 metres when the water depth reached 2.4 metres. The wave period did not show significant variation with increasing water depth. The average wave period was 8 seconds.

Suspended sediment concentration varies in phase tide level. Sediment concentration is related with water level by an exponential function $C / C_{max} = 0.107 \exp(0.6597D)$, where D is water depth. There is a remarkable variation of sediment concentration between the two main seasons. Sediment concentrations are much higher during the southerly winds than during the northerly winds. Long-shore sediment transport rates are found to be in the order of $3 \times 10^{-8} \text{ m}^3/\text{s}$ per linear meter along the beach.

Keywords: Sediment concentrations, eroding beach, nearshore currents

INTRODUCTION

The coast of Tanzania experiences a semi-diurnal tide with two almost equal maxima and two minima during a lunar day (24.8 solar hours). There is a considerable rise and fall of water (with a tidal range of 4.5 m) against the coast of Tanzania, which has important geomorphologic and hydrodynamic repercussions when combined with the intertidal profile and the prevailing winds. While the ebb and flood tidal movements tend to be self-balancing on the open coast, individual features will influence the extent of fluctuations. Tidal

currents in estuaries and areas with islands and sand spits such as at Kunduchi are localised and important in their effect on coastal topography.

Waves and currents along in the East African coastal waters are generally controlled by the seasonal monsoon winds. During the Northeast monsoon period when winds blow from the Northeast, the wind-generated waves approach the coast from the northerly sector and are likely to produce longshore currents with a southerly component. During the Southeast Monsoon, the wind direction is reversed and so is the wave and current climate. As such shoreline changes are also expected to be periodic in pattern and

intensity. The coastline of Tanzania north of Dar es Salaam City is generally exposed to both winds and there is very little shelter except for isolated islets and a fringing reef. Due to natural or human activities, there is severe beach erosion taking place in this area, which threatens properties and the land as a whole. This study aims at understanding aspects of some factors that contribute to the shoreline changes in this area.

STUDY AREA

The study area is the tidal flat off Kunduchi Beach, located approximately 10 kilometres north of Dar es Salaam City on the coast of Mainland Tanzania (Figure 1). In the vicinity of Kunduchi Beach, the main morphological features are the beach-ridge complex, which form backshore terraces and the shore-parallel

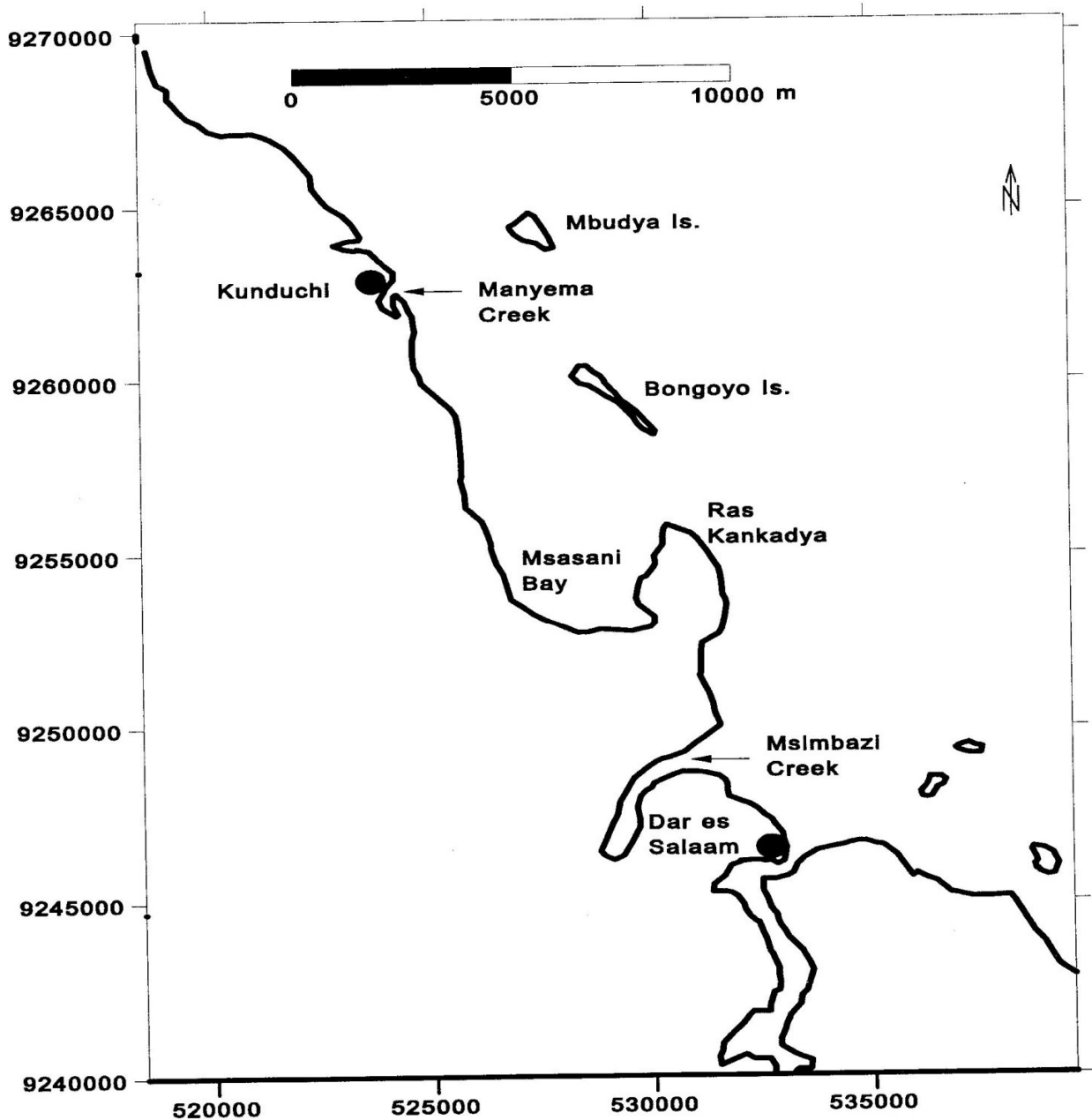


Figure 1: Location map of the study area

sand spits. There is an area of about 2 sq. km. of irregular sand deposits on the tidal flat. The most distinctive feature is a sand-spit, which is located immediately north of the outlet of the creek. The spit is reported to have been changing in shape and orientation over the years (Griffiths, 1987). The bathymetry off the beach shows that there are two submerged channels between the beach and the islands, which runs parallel to the coastline.

The general orientation of the shoreline is 330 degrees and the tidal flat is characterised by ripples. At about 150 m from the shoreline, ripples are 7-9 cm high and their wavelength is about 40 cm. Close to the beach, ripple orientation is 350 degrees; ripple height is 5 cm and ripple wavelength is 5 cm.

Measurements made during this study showed that during flood tide the current direction is southerly (an average of 210 degrees) and at high tide the average direction is 150 degrees. The direction of the ebb tidal current is northerly (an average of 360 degrees). On the average, the current speed was 0.1 m/s. Significant wave heights increased with increasing water level, from 0.1 metres in water depth of 0.5 metres to about 0.4 metres when the water depth reached 2.4 metres. The wave period did not show significant variation with increasing water depth. The average wave period was 8 seconds.

SEDIMENT SUSPENSION AND TRANSPORT ON THE TIDAL FLAT

Sediment transport modes can be split into three main types, namely bed load, suspended load and wash load. Bed load is understood to be that part of the load that is more or less continuously in contact with the bed during transport. The suspended load moves without continuous contact with the bed as a result of the agitation of fluid turbulence. The wash load consists of very fine particles which are transported by the water and which are normally not represented in the bed.

A considerable portion of the sediment transport in coastal areas is due to suspended sediment. According to Nielsen (1992) the sediment transport rate, through a unit width of a vertical

plane perpendicular to the x,u -direction, is usually given in the form

$$Q(t) = \int_0^D c(z,t) u_s(z,t) dz \quad (1)$$

$Q(t)$ has L^2T^{-1} . D is the total water depth, $c(z,t)$ is the local, instantaneous suspended sediment concentration and $u_s(z,t)$ is the instantaneous horizontal velocity of a sediment particle.

The time averaged sediment transport rate in the shore-parallel direction is given by

$$\bar{Q}_y = \int_{z=0}^D \bar{c}(z) \bar{v}(z) dz \quad (2)$$

where $\bar{c}(z)$ and $\bar{v}(z)$ are respectively time-average of suspended sediment concentration and horizontal velocity of the suspended sediment. In equation (2), it has been assumed that the transport perpendicular to the wave direction is dominated by $\bar{c}\bar{v}$. At elevations more than a centimetre or so above the bed, the suspended concentration equals the total sediment concentration and is therefore directly measurable.

The presence of waves changes the current velocity distributions. In a situation where data from a current meter is available, and if we know the wave amplitude A , angular frequency ω and current velocity $\bar{u}(z_r)$ at a position $z = z_r$ above the wave boundary layer, the current distribution can be derived. If we assume that the bed roughness and hence z_o is somehow known and z_r is within the logarithmic part of the current profile, the time averaged friction velocity is related to the current velocity (Nielsen, 1992) as

$$\bar{u}(z_r) = \frac{\bar{u}_*}{\kappa} \ln\left(\frac{z_r}{z_a}\right) = \frac{\bar{u}_*}{\kappa} \ln\left(\frac{z_r}{z_o F}\right) \quad (3)$$

where κ is von Karman's constant (≈ 0.4). The form of the function F is assumed known and following Sleath (1991), it is expressed as

$$F = \frac{z_a}{z_o} = 0.44 \frac{A\omega}{\bar{u}_*} \quad (4)$$

or

$$F = \frac{z_a}{z_o} = 1 + 0.19 \frac{A\omega}{\bar{u}_*} \sqrt{\frac{A}{r}} \quad (5)$$

where $z_o = r/30$ and $r = 8\eta^2/\lambda + 5\theta_{2.5}d$ is the hydraulic roughness, η is ripple height, λ is the ripple length, $\theta_{2.5}$ is the grain roughness Shields parameter and d is the grain size diameter. For the purpose of iteration, Equation (3) can be rearranged such that

$$\bar{u}_* = \frac{\kappa \bar{u}(z_r)}{\ln\left(\frac{z_r}{z_o}\right) - \ln\left(0.44 \frac{A\omega}{\bar{u}_*}\right)} \quad (6)$$

When the friction velocity \bar{u}_* has been found by iteration, the value of F can then be calculated and so can $z_a = z_o F$ and the thickness of the wave-dominated layer $l = e^1 z_a$. The velocity distribution of the current is then

$$\bar{u}(z) = \begin{cases} \frac{u_*}{\kappa} \ln\left(\frac{z}{z_a}\right) & \text{for } z > l \\ \frac{\bar{u}_*}{\kappa} \cdot \frac{z}{l} & \text{for } z < l \end{cases} \quad (7)$$

The initiation and eventually sediment transport are described by several parameters. The first parameter is the mobility number ψ , which is defined as the ratio of the total disturbing force $(A\omega)^2$ and the stabilising force due to gravity. This number is given as

$$\Psi = \frac{(A\omega)^2}{(s-1)gd} \quad (8)$$

where s is the relative density of sediment, g is the gravitational acceleration and d is the grain size diameter. The second measure of balance between the disturbing and stabilising forces on sand grains at the bed in a steady flow is the well-known Shields parameter given as

$$\theta = \frac{\tau(o)}{\rho(s-1)gd} = \frac{u_*^2}{(s-1)gd} \quad (9)$$

In a wave motion the Shields parameter can be expressed also in terms of the peak bed shear stress $\hat{\tau}$ as follows:

$$\theta = \frac{\hat{\tau}}{\rho(s-1)gd} = \frac{1/2 f_w (A\omega)^2}{(s-1)gd} = 1/2 f_w \psi \quad (10)$$

where f_w is the wave friction factor.

However, Madsen and Grant (1976) modified the mobility number ψ taking into account the ratio d/A of the force exerted by waves on sediment particles. As a result, the sediment mobility is measured in terms of the *grain roughness* Shields parameter. For flat beds of sand with median size d_{50} , the grain roughness Shields parameter $\theta_{2.5}$ is given as

$$\theta_{2.5} = \frac{1/2 f_{2.5} \rho (A\omega)^2}{\rho(s-1)gd} = 1/2 f_{2.5} \psi \quad (11)$$

where $f_{2.5}$ is the special grain roughness friction factor based on Swart's (1974) formula.

$$f_{2.5} = \exp\left[5.213 \left(\frac{2.5d_{50}}{A}\right)^{0.194} - 5.977\right] \quad (12)$$

For rippled beds, θ is generally an order of magnitude greater than $\theta_{2.5}$ with no systematic trend between different sizes.

The ripple geometry is described by the ripple length λ and ripple height η . For field conditions, Nielsen (1981) suggested the following relations

$$\frac{\lambda}{A} = \exp\left(\frac{693 - 0.37 \ln^8 \psi}{1000 + 0.75 \ln^7 \psi}\right) \quad (13)$$

$$\frac{\eta}{A} = 21\psi^{-1.85} \quad (14)$$

$$\frac{\eta}{\lambda} = 0.342 - 0.344\sqrt{\theta_{2.5}} \quad (15)$$

The distribution of the time-averaged sediment concentrations is given by a simple exponential formula as

$$\bar{c}(z) = C_o e^{-z/L_s} \quad (16)$$

where z is measured in metres above the ripple crest level. C_o is known as the reference concentration and is given by

$$C_o = 0.005 \frac{\theta_{2.5}^3}{(1 - \pi\eta / \lambda)^6} \quad (17)$$

and L_s is the distribution length scale given by

$$L_s = 0.075 \frac{A\omega}{w_o} \eta \quad (18)$$

where w_o is the fall velocity given by

$$w_o = \frac{(s-1)gd^2}{18\nu} \quad (19)$$

in which ν is the kinematic viscosity with a typical value = 1×10^{-6} (m^2/s).

FIELD MEASUREMENTS

Currents were measured using an Aanderaa self-recording current meter model 9 (RCM9). The current meter was deployed in March/April for one month during the NE-monsoon and again in August/September for another month during the SE-monsoon in 1998. The current meter is a self-contained instrument that can be moored in the sea for long periods of time. It measures the horizontal current speed and direction, temperature, conductivity and turbidity as well as pressure from which we can get the

instrument's depth. The instrument has an optional channel for an additional sensor.

The instrument was deployed on the tidal flat 4.13 metres below the benchmark and approximately 118.5 metres from the beach dune. It was mounted on a 1.2-metre long, 20cm wide x 5cm thick hard wooden plank. On each end of the plank, another 1.2-metre long 10cm x 5 cm piece of hard wood was bolted to make an I - frame. The design, plus added weights of two standard sand/cement blocks, ensured stability against overturning during the passage of waves and currents. When deployed, the sensors are 0.5 m above the ground. A pressure gauge for measuring waves was deployed near the RCM9.

RESULTS AND DISCUSSION

Variation of sediment concentration and current speed with water level and time

During the southerly monsoon winds (June-October), wave activity is more intense than during the northerly monsoon winds. Figure 2 shows that in September the morning and evening patterns of sediment concentration are different. In the evenings, sediment

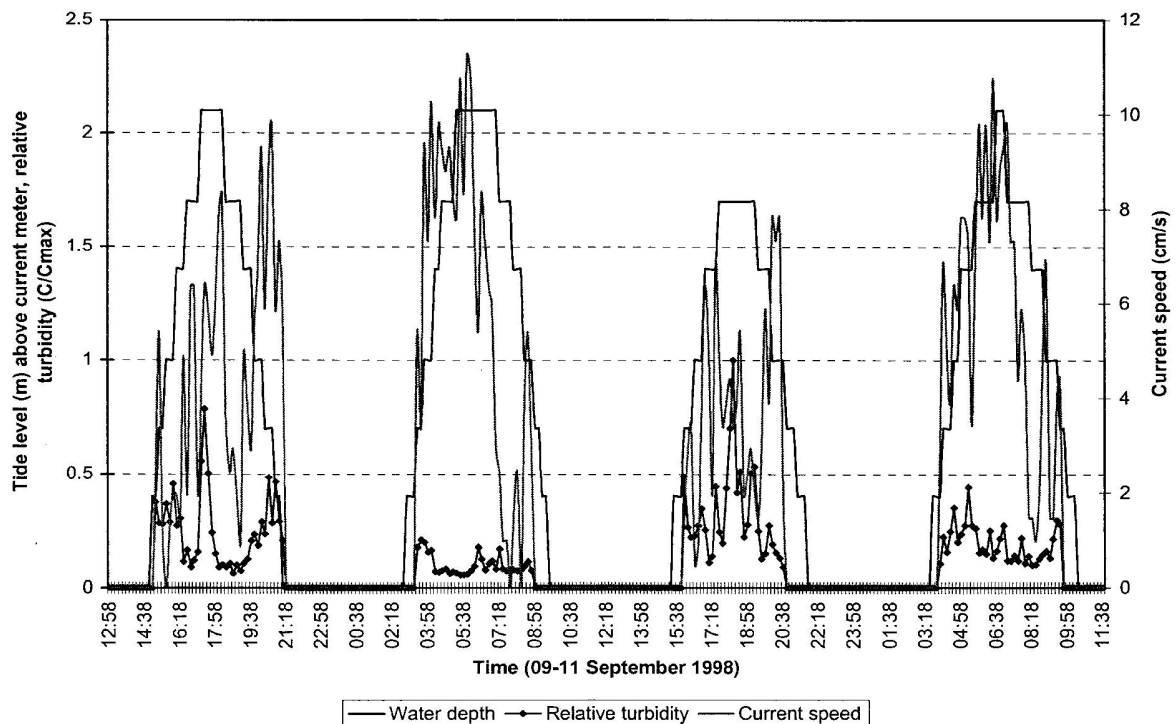


Figure 2: Variation of water level, currents and sediment concentration with time

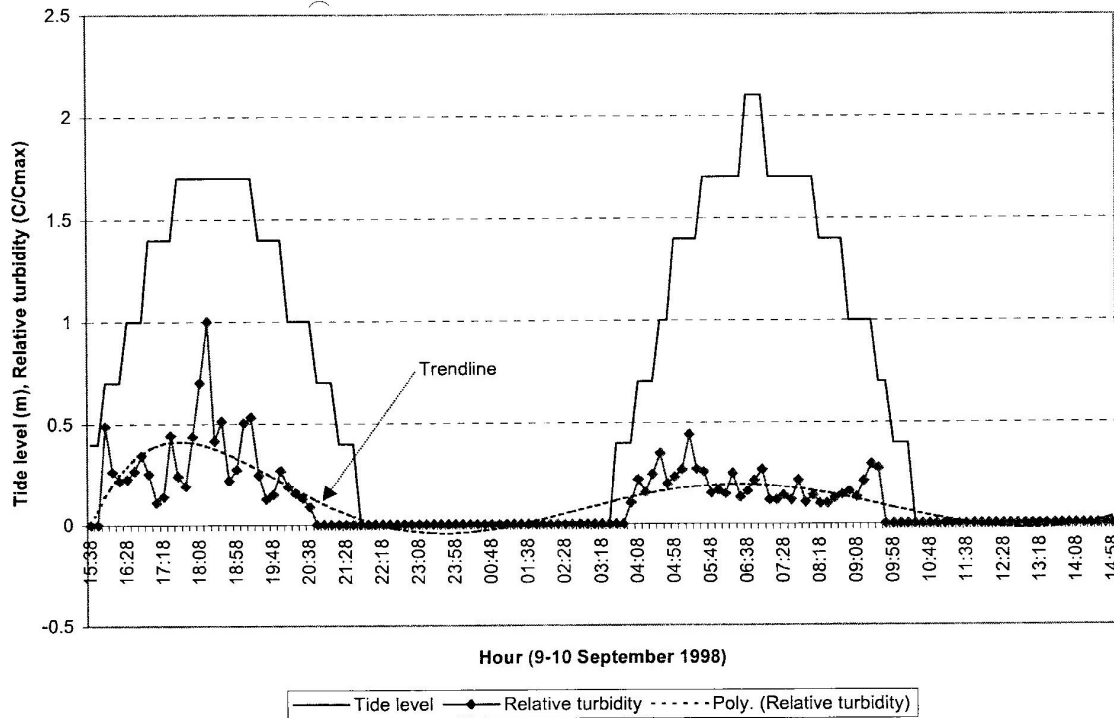


Figure 3: Patterns of current and sediment concentrations.

concentration is higher than those in the mornings and the highest peaks occur during high water in the evenings, when winds are strongest. Morning currents are highest before high water, while evening currents are highest

after high water.

Sediment concentration varies in phase with tide level (Figure 3), such that it can be represented by

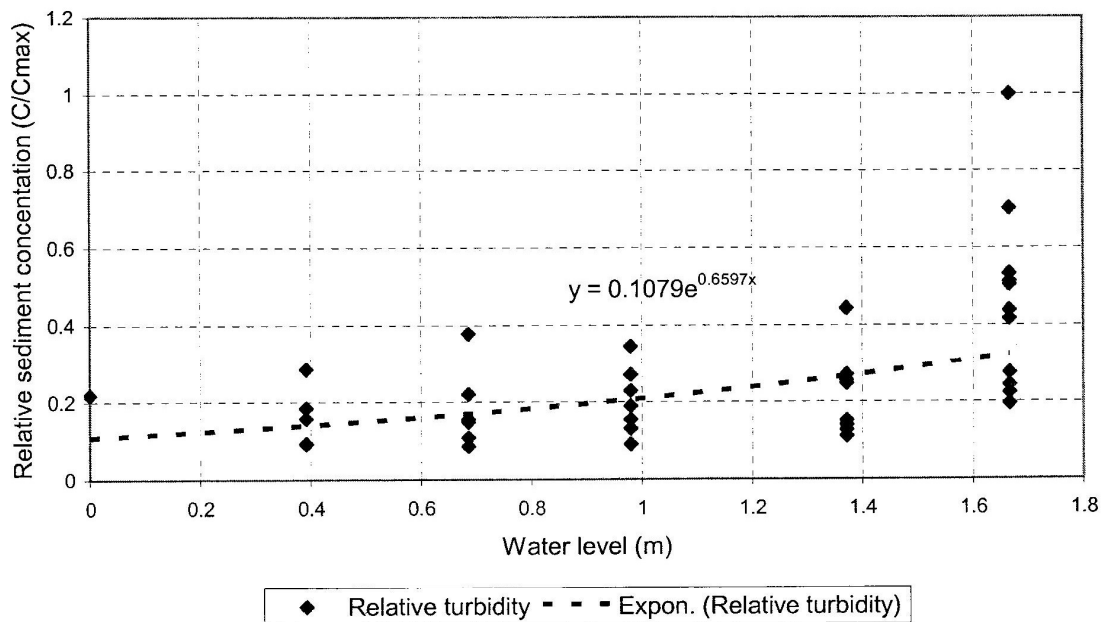


Figure 4: Variation of sediment concentration with water level

Table 1: Current, wave parameters and sediment transport rate

	Case 1	Case 2	Case 3	Case 4	Case 5	Case 6
Water depth (m)	1.1	1.2	1.3	1.7	2.2	2.4
H _{mo} (m)	0.23	0.27	0.14	0.21	0.41	0.45
T _p (s)	12	11	10	11	10	11
C _o	9.1775e-6	1.8266e-5	2.0771e-6	6.0568e-6	6.4827e-5	7.7243e-5
L _s (m)	0.016	0.011	0.024	0.017	0.007	0.007
Aω (m/s)	0.2431	0.2787	0.1692	0.2183	0.3632	0.3836
η (m)	0.0483	0.0306	0.1072	0.0592	0.0136	0.0129
λ (m)	0.3072	0.2113	0.5917	0.3602	0.1136	0.1113
z _o	0.0020	0.0012	0.0052	0.0026	0.0004	0.0004
\bar{u}_* (m/s)	0.012	0.0110	0.0139	0.0124	0.0093	0.0094
r	0.0610	0.0357	0.1555	0.0780	0.0133	0.0123
l	0.1087	0.1246	0.0756	0.0976	0.1624	0.1715
l/L _s	3.1406	3.1539	3.1251	3.1624	3.1278	3.0072
\bar{Q}_y (m ³ /s/m)	2.946e-8	2.735e-8	2.631e-8	2.739e-8	2.531e-8	2.912e-8

$$c = c_{max} \sin \omega t \tag{20}$$

where c is the instantaneous concentration and c_{max} is the concentration amplitude, $\omega = \frac{2\pi}{T}$ and $T = 12.6$ hours is the tide wave period. A closer look at Figure 3 reveals that sediment suspension is maximum in the middle of flooding, at high water and in the middle of ebbing.

The current speed has two peaks; one is found at mid-flooding and the other at mid-ebbing (Figure 2). It is lowest at high tide, such that it can be represented by

$$u = u_{max} \sin \frac{\omega}{2} t \tag{21}$$

where u_{max} is the amplitude of the current speed. Figure 4 shows that sediment concentration is exponentially related to water level.

The current profile and rate of sediment transport

During the southerly monsoons, waves passing the tidal flat of Kunduchi at high tide are of height of the order 0.1-0.5 m, such that they break directly on the beach slope. The current profile and the product, $\bar{c}(z)\bar{v}(z)$, are found using the linear wave theory and the measured wave, current and sediment parameters, i.e.

($H_{mo}, T_p, \bar{v}(z_r), d_{50}, w_o, s$) as shown in Table 1. Inserting Equation (16) and Equation (17) into Equation (2), the time averaged sediment transport rate is calculated as

$$\bar{Q}_y = \int_0^D \bar{c}(z)\bar{v}(z)dz = \frac{C_o \bar{v}_*}{\kappa d} \int_0^l z e^{-z/L_s} dz + \frac{C_o \bar{v}_*}{\kappa} \int_l^D \ln \frac{z}{z_a} e^{-z/L_s} dz \tag{22}$$

In the present cases, l/L_s is greater than 2 (see Table 1) and according to Nielsen (1992), the second term of Equation (22) can be neglected, such that the sediment transport rate is approximated as

$$\bar{Q}_y \approx \frac{\bar{v}_*}{\kappa} C_o \frac{L_s^2}{l} \tag{23}$$

Table 1 shows the calculated values according to Equation (23). Figure 4 shows variation of sediment concentration with water level. Using the least squares method, curve fitting to the measured data shows that sediment concentration is related to the water level by an exponential function $C/C_{max} = 0.107 \exp(0.6597D)$, where D is the water depth. Figure 5 shows the distribution of the product $\bar{c}(z)\bar{v}(z)$ for three cases of wave parameters.

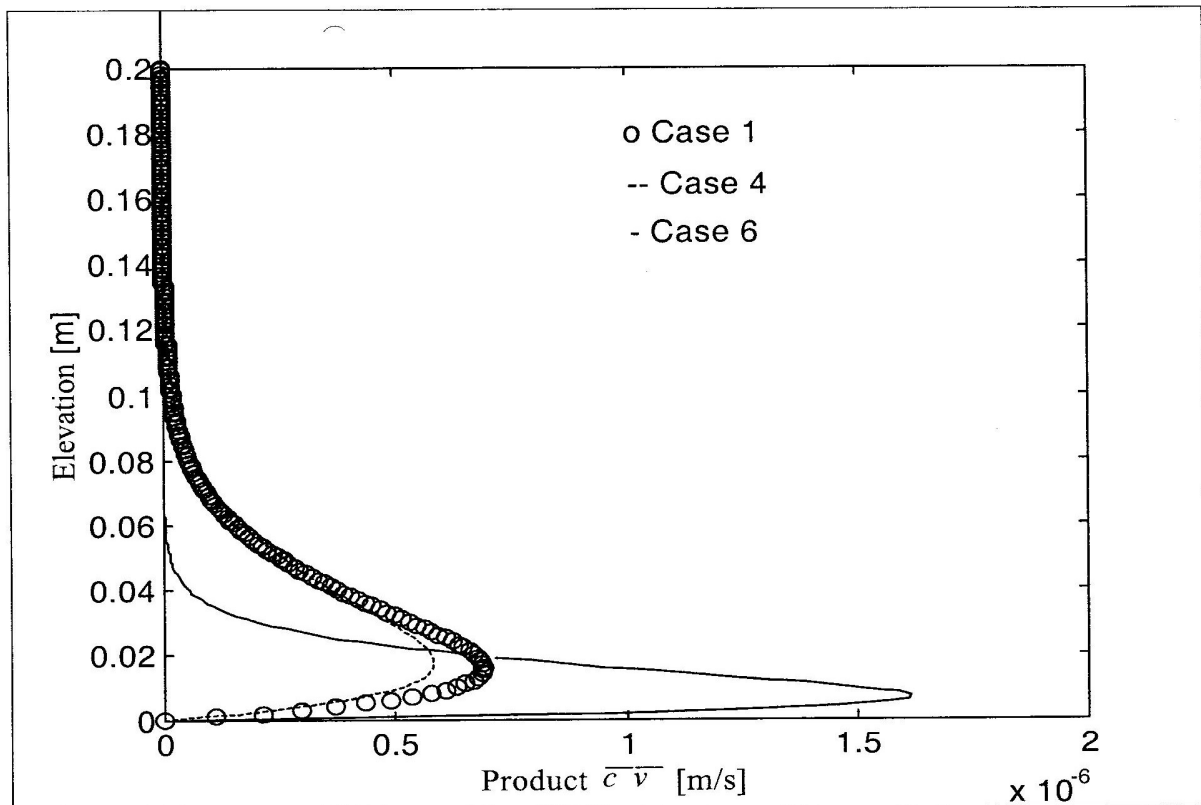


Figure 5: Distribution of the product $\bar{c}\bar{v}$ for three cases in Table 1.

CONCLUSION

From Table 1, we see that the calculated ripple height ranges from 1.3 cm to about 6 cm, which correspond to the measured heights close to the beach. The ripple wavelengths vary between 11 cm and 60 cm, which also correspond with the measured ones. Waves and currents vary in energy on a seasonal and even daily basis and so is their capacity to move sediment. Although Figure 4 shows that sediment increases exponentially with water level, it should be noted that it is at high water that the most energetic waves reach the tidal flat. This is evidenced when we compare sediment concentrations in the two high water levels in Figure 3. Although the second high water is greater than the first, sediment concentrations are lower than in the first. During the southerly winds, ebbing tide will coincide with waves and thus increase the transport rate of the already suspended sediment at high water. During a complete tidal cycle, the ebbing currents will carry away an average of 1.27 m^3 of sediments from a beach of one kilometre long. Given the

profile of the beach and with long-term measurements of the wave and current parameters, actual sediment erosion and consequently shoreline erosion can be determined.

NOTATION

- A wave amplitude
- C_o reference sediment concentration
- c_{max} sediment concentration amplitude
- $c(z,t)$ is the local, instantaneous suspended sediment concentration
- $u_s(z,t)$ is the instantaneous horizontal velocity of a sediment particle.
- $\bar{c}(z)$ time-average of suspended sediment concentration
- D is the total water depth,
- d sediment grain diameter

d_{50}	median grain diameter
$\bar{v}(z)$	time-average horizontal velocity of the suspended sediment.
$f_{2.5}$	grain roughness friction factor
f_w	wave friction factor
g	gravitational acceleration
l	thickness of wave-dominated layer
L_s	scale of suspended sediment distribution
$Q(t)$	is transport rate having dimension L^2T^{-1}
r	the hydraulic roughness
s	relative density of sediment
T	Tide wave period (12.6 hours)
\bar{u}_*	average friction velocity, $ \bar{u}_* \bar{u}_* = \tau_o / \rho$
$\bar{u}(z_r)$	time-average of current velocity at a position $z = z_r$ above the wave boundary layer
w_o	sediment fall velocity
z_o	zero-intercept level of log velocity profile due to current alone
z_a	zero-intercept level of log velocity profile due to combined wave and current flow
z_r	level of reference current
λ	ripple length
η	ripple height
θ	Shields parameter
$\theta_{2.5}$	grain roughness Shields parameter
κ	von Karman's constant (≈ 0.4)

ν	kinematic (laminar) viscosity
ρ	fluid density
$\tau(o)$	bed shear stress
$\hat{\tau}$	peak bed shear stress under waves
ψ	the mobility number
ω	angular frequency and current velocity, the current distribution can be derived.

REFERENCES

1. Griffiths, C.J., *The impact of sand extraction from seasonal streams on erosion of Kunduchi*. In: Beach Erosion Monitoring Committee. "Beach Erosion Along Kunduchi Beach, North of Dar Es Salaam". Report for National Environment Management Council, 1987, pp. 36-47
2. Madsen, O.S. and W.D. Grant, "*Sediment transport in the coastal environment*". Report No. 209, Palph M. Parsons Lab., MIT, 1976
3. Nielsen, P. "*Dynamics and geometry of wave generated ripples*", J. Geophys. Res. Vol. 86, No. C7, (1981), pp. 6467-6472,
4. Nielsen, P. "*Coastal Bottom Boundary Layers and Sediment Transport*", Advanced Series on Ocean Engineering - Volume 4. World Scientific Publishing Co. Pte. Ltd., Singapore, 1992, 324 p.
5. Sleath, J.F.A., "*Velocities and shear stresses in wave-current flows*" J. Geophys. Res., Vol. 96, No. C8, 1991, pp. 15237-15244.